Human Genetics (2019) 138:231–239
https://doi.org/10.1007/s00439-019-01980-3

ORIGINAL INVESTIGATION

PUS7 mutations impair pseudouridylation in humans and cause intellectual disability and microcephaly

Ranad Shaheen[1] · Monika Tasak[2] · Sateesh Maddirevula[1] · Ghada M. H. Abdel-Salam[3,4] · Inas S. M. Sayed[5] · Anas M. Alazami[1] · Tarfa Al-Sheddi[1] · Eman Alobeid[1] · Eric M. Phizicky[2] · Fowzan S. Alkuraya[1,6,7]

Received: 31 December 2018 / Accepted: 7 February 2019 / Published online: 18 February 2019

Abstract

Pseudouridylation is the most common post-transcriptional modification, wherein uridine is isomerized into 5-ribosyluracil (pseudouridine, Ψ). The resulting increase in base stacking and creation of additional hydrogen bonds are thought to enhance RNA stability. Pseudouridine synthases are encoded in humans by 13 genes, two of which are linked to Mendelian diseases: *PUS1* and *PUS3*. Very recently, *PUS7* mutations were reported to cause intellectual disability with growth retardation. We describe two families in which two different homozygous *PUS7* mutations (missense and frameshift deletion) segregate with a phenotype comprising intellectual disability and progressive microcephaly. Short stature and hearing loss were variable in these patients. Functional characterization of the two mutations confirmed that both result in decreased levels of Ψ_{13} in tRNAs. Furthermore, the missense variant of the *S. cerevisiae* ortholog failed to complement the growth defect of *S. cerevisiae pus7Δ trm8Δ* mutants. Our results confirm that *PUS7* is a bona fide Mendelian disease gene and expand the list of human diseases caused by impaired pseudouridylation.

Keywords Pseudouridylation · Microcephaly · *PUS7*

Introduction

Ribonucleosides undergo more than 160 modifications (Boccaletto et al. 2017). These modifications influence the stability and function of RNAs, and in some cases are thought to play a key role in the dynamic control of gene expression (Endres et al. 2015; Hoernes et al. 2016; Jackman and Alfonzo 2013; Motorin and Helm 2010; Zhao et al. 2017). The most common of these post-transcriptional modifications (PTMs) is pseudouridylation, wherein uridine is isomerized into 5-ribosyluracil (pseudouridine, Ψ) (Charette and Gray 2000). Pseudouridine was first identified in 1951 and was originally referred to as the "fifth" nucleoside before its identity as 5-ribosyluracil was determined later (Cohn 1959; Cohn and Volkin 1951). Pseudouridylation has been documented in all three major RNA species (tRNA, rRNA

Ranad Shaheen, Monika Tasak, and Sateesh Maddirevula have contributed equally.

Electronic supplementary material The online version of this article (https://doi.org/10.1007/s00439-019-01980-3) contains supplementary material, which is available to authorized users.

✉ Eric M. Phizicky
eric_phizicky@urmc.rochester.edu

✉ Fowzan S. Alkuraya
falkuraya@kfshrc.edu.sa

1 Department of Genetics, King Faisal Specialist Hospital and Research Center, Riyadh, Saudi Arabia

2 Department of Biochemistry and Biophysics, Center for RNA Biology, University of Rochester School of Medicine and Dentistry, Rochester, NY, USA

3 Clinical Genetics Department, Human Genetics and Genome Research Division, National Research Centre, Cairo, Egypt

4 Human Cytogenetics Department, Human Genetics and Genome Research Division, National Research Centre, Cairo, Egypt

5 Oro-dental Genetics Department, Human Genetics and Genome Research Division, National Research Centre, Cairo, Egypt

6 Saudi Human Genome Program, King Abdulaziz City for Science and Technology, Riyadh, Saudi Arabia

7 Department of Anatomy and Cell Biology, College of Medicine, Alfaisal University, Riyadh, Saudi Arabia

and mRNA) as well as in snRNA and snoRNA (Andrew et al. 2011; Branlant et al. 1981; Carlile et al. 2014; Grosjean et al. 1995; Li et al. 2015; Lovejoy et al. 2014; Schattner et al. 2006; Schwartz et al. 2014; Boccaletto et al. 2017). The reason for the abundance of pseudouridine is incompletely understood, but is thought to be driven by its advantageous effect on RNA stability by virtue of improved base stacking and the creation of additional hydrogen bonds (Davis 1995; Spenkuch et al. 2014).

Six families of enzymes are known to synthesize pseudouridine (pseudouridine synthases or PUS enzymes): TruA, TruB, TruD, RsuA, RIuA, and Pus10b. With the exception of RsuA, these families are represented in humans by pseudouridine synthases encoded by 13 genes, some of which represent paralogs such as *PUS1*/*PUS1L, TRUB1*/*TRUB2*, and *PUS7*/*PUS7L* (Spenkuch et al. 2014). Human PUS enzymes are far less studied than their counterparts in other organisms. However, recent advances in human Mendelian diseases have brought renewed focus on these enzymes and their relevance to clinical medicine. The first human disease linked to PUS genes was myopathy, lactic acidosis, and sideroblastic anemia 1 (MLASA1) (MIM 600462), which was found to be caused by biallelic mutations in *PUS1* (Fernandez-Vizarra et al. 2007). In 2016, we described a novel intellectual disability and microcephaly syndrome in three affected siblings who all shared a homozygous truncating variant in *PUS3* (Shaheen et al. 2016). In addition, we recently encountered a patient with severe global developmental delay and epilepsy with a homozygous truncating variant in *PUS7L* (manuscript under review). These findings suggest that PUS genes are attractive candidates for Mendelian diseases in humans and raise interesting questions about the nature and extent of the associated phenotypes.

In this study, we describe two consanguineous families each segregating a different likely deleterious homozygous variant in *PUS7* (one missense and one frameshift deletion). The associated phenotype is consistent and comprises severe intellectual disability and progressive microcephaly. Both variants were associated with a specific reduction of Ψ_{13} in their tRNAs. Our findings are compatible with one study that was published in the course of preparing this manuscript and provide independent confirmation of this novel *PUS7*-related syndrome (de Brouwer et al. 2018).

Materials and methods

Human subjects

The two study families were enrolled in an IRB-approved research protocol (RAC#2080006) and informed consent was obtained. All three patients were evaluated by board-certified clinical geneticists, and full phenotypic data were collected from their medical records. In addition to the patients, their parents and available siblings were also included in the study. Venous blood was collected in EDTA and in sodium heparin tubes for DNA extraction and the establishment of lymphoblastoid cell lines (LCLs), respectively.

Positional mapping, exome sequencing, and variant interpretation

Chromosome analysis (karyotyping) and molecular karyotyping were performed for the three patients and were negative. The molecular karyotyping was performed using CytoScan HD array platform (Affymetrix) that contains 2.6 million markers for CNV detection, of which 750,000 are genotyping SNPs and 1.9 million are non-polymorphic probes. DNA samples were genotyped using the Axiom SNP Chip platform following the manufacturer's instructions. Autozygome was mapped based on regions of homozygosity > 2 Mb as surrogates of autozygosity given the parental consanguinity followed by mapping of the candidate autozygome that is exclusively shared by the affected members using AutoSNPa. Linkage analysis was used to confirm the candidate autozygome and calculate LOD score based on a fully penetrant autosomal recessive model using the EasyLINKAGE package.

Exome capture was performed using the TruSeq Exome Enrichment kit (Illumina, San Diego, CA, USA) as per the manufacturer's instructions. Samples were prepared as an Illumina sequencing library, and in the second step, the sequencing libraries were enriched for the desired target using the Illumina Exome Enrichment protocol. Captured libraries were sequenced using Illumina HiSeq 2000 Sequencer, and the reads mapped against UCSC hg19 (http://genome.ucsc.edu/) by BWA (http://bio-bwa.sourceforge.net/). The SNPs and Indels were detected by SAMTOOLS (http://samtools.sourceforge.net/). The resulting variants were filtered as follows: homozygous → coding/splicing → within candidate autozygome → absent or very rare in Saudi and public exome databases → predicted to be pathogenic by SIFT/PolyPhen/CADD as previously described (Alkuraya 2013).

Extraction of total RNA and purification of tRNA from human cells

Lymphoblastoid cell lines were grown at 37 °C in 5% CO_2 in RPMI 1640 medium containing FBS (15%), penicillin (1 U/mL), streptomycin (1 µg/mL), and amphotericin b (0.5 µg/mL) to a density of ~ 1.0×10^6 cells/mL, and then, 2.5 mL was used to generate triplicate cultures. Bulk RNA from ~ 3.6×10^8 cells was extracted with TRIzol (Life Technologies) according to manufacturer's instructions. Then, $tRNA^{Val(AAC)}$ was purified

from 1 to 1.25 mg bulk RNA using a 5′ biotinylated oligonucleotide (Integrated DNA Technologies) complementary to nucleotides 53–76, digested with P1 nuclease and phosphatase, and nucleosides were analyzed by HPLC, as previously described (Jackman et al. 2003).

Analysis of Ψ_{13} of tRNA

Bulk RNA obtained from LCLs was analyzed for Ψ_{13} by treatment with *N*-cyclohexyl-*N*′-(2-morpholinoethyl)carbodiimide methyl-*p*-toluenesulfonate (CMCT, also called CMC), followed by primer extension, essentially as previously described (Huang et al. 2016). Incubation of bulk RNA with CMCT was followed by alkaline treatment, and then RNA was annealed with 5′ ^{32}P-labeled primers that hybridized to nucleotides 40–23 of $tRNA^{His(GTG)}$ or 39–21 of $tRNA^{Glu(CTC)}$, and reverse transcribed with AMV polymerase (Promega). Products were then resolved on a 15% polyacrylamide-7M urea gel and imaged by a phosphorimager.

Yeast strains and plasmids

To construct a *CEN* plasmid expressing *Saccharomyces cerevisiae PUS7* from its own promoter, *PUS7* DNA was amplified from yeast genomic DNA with primers hybridizing 853 nucleotides upstream and 253 nucleotides downstream of the open reading frame, and then cloned into a (*URA3 CEN*) vector. Plasmid EMT082-1 expressing the *S. cerevisiae* Pus7-D478Y variant (homologous to the human PUS7-D503Y variant) was generated by QuickChange PCR according to manufacturer's instructions (Stratagene), and the resulting plasmid was sequenced before use. Yeast strains with [*URA3*] plasmids were grown in S-Ura minimal medium or rich (YPD) media, as indicated (Sherman 1991).

Results

Clinical report

Three affected individuals from two consanguineous families are included in this study (Fig. 1A). The full clinical reports describing the phenotype of the three patients are in Table S1 and representative clinical photos are shown in Fig. 1A. Several clinical phenotypes are shared among the affected patients including microcephaly, intellectual disability (ID), aggressive behavior, and speech delay in addition to dysmorphic features such as smooth philtrum and everted lower lip (Table 1; Fig. 1A).

PUS7 is mutated in an autosomal recessive syndrome of intellectual disability and microcephaly

Each family was analyzed independently initially. In Family 1, three novel variants that are predicted deleterious in silico were identified in genes linked to the autozygome of the index: *PUS7* [NM_019042.3:c.1507G>T, p. (Asp503Tyr)], *GDF9* [NM_005260.5:c.947G>A, p. (Arg316His)] and *TRIM4* [NM_033017.3: c.337C>T, p. (Gln113*)]. In Family 2, however, only one novel variant that is predicted deleterious was identified within the candidate autozygome: a four base pair deletion in *PUS7* gene (NM_019042.3:c.329_332delCTGA). Based on the latter finding and the similarity in the phenotypes (intellectual disability and microcephaly) between the three patients, we prioritized *PUS7* [NM_019042.3:c.1507G>T, p. (Asp503Tyr)] in Family 1 for functional validation. It should be noted that the missense variant p. (Asp503Tyr) is located within the TRUD domain (the pseudouridine catalytic domain of PUS7), predicted to be probably damaging (1) by Polyphen-2, deleterious by SIFT (0), "disease causing" by MutationTaster and has a CADD_phred of 29.4. The truncating variant c.329_332delCTGA is predicted to remove 551 amino acids from the protein, leading to complete absence of the TRUD domain (370–580) (Fig. 1C). Both variants fully segregated with the phenotype in each family (Fig. 1A). In addition, an LOD score of 3.4 for the locus chr7: 96,488,196–109,035,887 (hg19) spanning *PUS7* was obtained when combining the two families (Fig. 1D).

Human mutations in *PUS7* result in decreased levels of Ψ_{13} in tRNAs.

Since *S. cerevisiae PUS7* encodes the pseudouridine synthase that catalyzes pseudouridine formation at U_{13} in yeast cytoplasmic tRNAs, as well as at U_{35} in pre-$tRNA^{Tyr(GUA)}$ (Behm-Ansmant et al. 2003), we analyzed characterized human tRNAs known to have Ψ_{13} from the three patient LCLs (IV:1, IV:2, IV:3) and from control LCLs. We specifically analyzed Ψ_{13} using the well-established CMCT assay, which detects Ψ as a primer extension pause after CMCT treatment (Bakin and Ofengand 1993; Huang et al. 2016). Our CMCT analysis showed that $tRNA^{His(GTG)}$ and $tRNA^{Glu(CTC)}$ from LCLs of patients with the Asp503Tyr mutation lacked Ψ_{13} (Fig. 2a), whereas each of two control LCLs had a prominent pause corresponding to the Ψ_{13} modification. Similarly, $tRNA^{Glu(CTC)}$ from an LCL from a patient with Thr110Argfs*4 mutation lacked Ψ_{13}, compared to a control LCL (Fig. 2b).

To quantify the defect in Ψ_{13} modification of tRNA due to the Asp503Tyr missense mutation (Fig. 1C), we purified $tRNA^{Val(AAC)}$ and analyzed its nucleosides by HPLC.

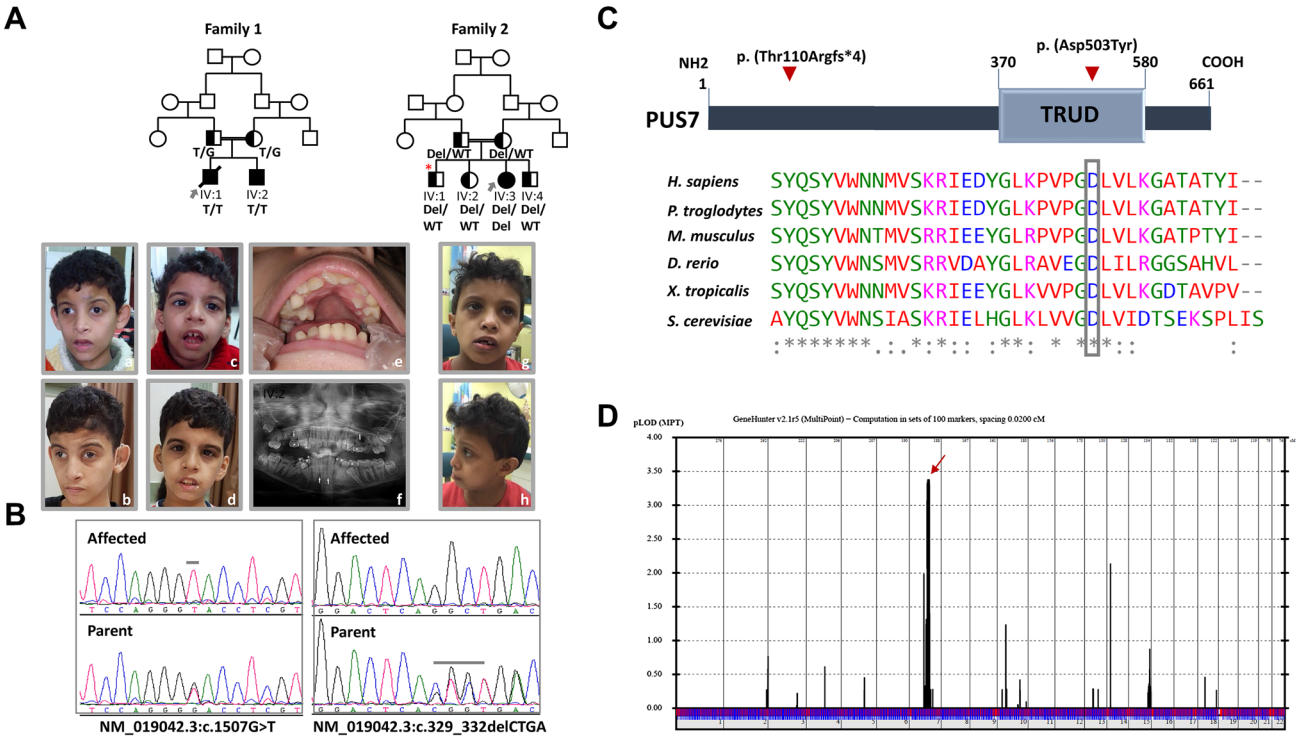

Fig. 1 *PUS7* mutations cause intellectual disability and microcephaly. **A** Upper panel: families pedigrees of 12DG2083 and 12DG2084 (Family 1) and 16DG0965 (Family 2) showing the consanguineous nature of the parents. The index is indicated in each pedigree by grey arrow, and segregation analysis denoted by half black color [heterozygous for recessive allele (carrier)]. Red star denotes sibling with resolved hydrocephalus. Lower panel: the facial photos of the affected individuals in this study and the dental photo and panoramic radiograph of the index 12DG2084. *a* and *b* Facial photos of the index IV:1 (12DG2083) at the age 9 years and 16 years showing the dysmorphic features seen in the patient (smooth philtrum, everted lower lip, triangular face, prominent glabella, arched eyebrows, deep-set eyes, infraorbital crease, convergent squint, hypoplastic zygomatic arches, anteverted nostrils and prominent ears with simple helix). *c* and *d* Facial photos of IV:2 (12DG2084) at the age of 7 and 14 years showing the dysmorphic features observed in the patient (smooth philtrum, everted and thick lower lip, deep-set eyes and infraorbital crease, downward slanting of eyes and low set ears). *e* and *f* Intraoral and panoramic radiographs of the patient 12DG2084 showing multiple retained deciduous teeth (asterisks in f), malpositioned permanent teeth and congenitally missing lower permanent lateral incisors and upper second premolars (arrows). *g* and *h* Facial photos of the index IV:3 (16DG0965) at the age of 8 years showing the dysmorphic features of the patient (microcephaly, smooth philtrum, mildly upturned nares and everted lower lip). **B** Sequence chromatograms showing the homozygous variants in *PUS7* in the index of each family and the heterozygous parents. **C** Upper panel is the schematic of PUS7 showing the position of domain "TRUD" and the location of the two variants p. (Thr110Argfs*4) and p. (Asp503Tyr). Lower panel showing multisequence alignment of the mutated reside p. (Asp503) showing the conservation down to *S. cerevisiae* (boxed in grey). **D** Genome-wide linkage analysis to the two families revealed a single maximal peak with an LOD score of ~ 3.4 on chromosome 7

We chose $tRNA^{Val(AAC)}$, because it only had two other pseudouridine residues in addition to Ψ_{13}, and because it was amenable to purification (Shaheen et al. 2015). $tRNA^{Val(AAC)}$ purified from the LCL from patient IV:2 with the Asp-503Tyr mutation showed a reduction of 0.88 mol of Ψ relative to that from a WT control (1.75 mol/mol compared to 2.63 mol/mol). By contrast, the levels of the other analyzed $tRNA^{Val(AAC)}$ modifications (m^5C, m^2G) were very similar between the patient and control LCLs (Fig. 3; Table 2). Thus, our results strongly suggest that PUS7 with either the Asp503Tyr mutation or the Thr110Argfs*4 mutation is severely deficient in the isomerization of U_{13} to Ψ, linking this defect to the ID, consistent with the known biological effects of PUS7 (see below).

Expression of *S. cerevisiae pus7-D503Y* does not complement the growth defect of *S. cerevisiae pus7Δtrm8Δ* mutants

We used *S. cerevisiae* as a model to further analyze the effects of the PUS7-Asp503Tyr missense mutation, since the Thr110Argfs*4 mutation is an apparent loss of function truncating variant. We generated a low copy (*CEN*) plasmid expressing *S. cerevisiae pus7- D478Y* (equivalent to human *PUS7-D503Y*) from its native promoter [*CEN URA3* P_{PUS7}-*pus7-D478Y*] to test its ability to complement the severe slow growth defect of an *S. cerevisiae pus7Δ* mutant strain in a *trm8Δ* background which, as reported previously, grows very poorly at 33 °C and higher

Table 1 Clinical phenotype of patients with *PUS7* mutations

Family	Family 1 (this study)		Family 2 (this study)	1 (PKMR215) de Brouwer et al. (2018)			2 (MR046) de Brouwer et al. (2018)		3 (R14-22173) de Brouwer et al. 2018)
Case ID	12DG2083	12DG2084	16DG0965	IV-2	IV-3	IV-4	IV-1	IV-2	II-2
Variant NM_019042.3	c.1507G>T, p. (Asp503Tyr)		c.329_332delCTGA, p. (Thr110Argfs*4)	c.89_90del, p. (Thr30Lysfs*20)			c.1348C>T, p. (Arg450*)		Exon 15 deletion
Sex	M	M	F	F	M	M	M	M	M
Ethnicity	Egyptian	Egyptian	Saudi	Pakistani	Pakistani	Pakistani	Syrian	Syrian	Moroccan
Consanguinity	Y	Y	Y	Y	Y	Y	Y	Y	Y
Age at last examination	16 years	14 years	6 years	18 years	14 years	7 years	8 years	2 years	3 years 3 months
Growth at birth									
OFC (cm)	ND	ND	ND	ND	ND	ND	ND	ND	ND
Height (cm)	ND	ND	ND	ND	ND	ND	ND	ND	ND
Weight (kg)	1.5 (−3 SD)	2.5 (−2 SD)	ND	ND	ND	ND	ND	ND	ND
Growth at the last examination									
OFC (cm)	46 (−6 SD)	44.5 (−6.7 SD)	45.3 (−4.5 SD)	50 (−4.0 SD)	49 (−3.6 SD)	ND	46.5 (−4.5 SD)	46 (−2.5 SD)	46.3 (−2.5 SD)
Height (cm)	145 (−4 SD)	125 (−6.6 SD)	112.5 (33rd centile)	140 (<−3.9 SD)	137 (<− 3.5 SD)	ND	104 (−4.0 SD)	80 (−2.2 SD)	95.5 (−2.2 SD)
Weight (kg)	32 (−3 SD)	21 (−3.7 SD)	18.3 (20th centile)	37 (−3.6 SD)	29.5 (−3.2 SD)	ND	ND	ND	11.5 (−3.0 SD)
Neurological									
Intellectual disability (level)	+ (Moderate)	+ (Moderate)	+ (Severe)	+ (Moderate)	+ (Moderate)	+ (Moderate)	+ (Moderate)	+ (Moderate)	+ (Moderate)
Motor delay	+	+	−	−	−	−	+	+	+
Speech delay	+	+	+	+	+	+	+	+	+
Behavioral problems	Aggressive	Aggressive	Aggressive	Aggressive	Aggressive	Aggressive	Aggressive	ND	Aggressive
Dysmorphic	Short smooth philtrum Everted lower lip Triangular face Prominent glabella Arched eyebrows Deep-set eyes Infraorbital crease Convergent strabismus Hypoplastic zygomatic arches Anteverted nares Prominent ears with simple helix High arched palate with narrow vault Wide overjet, deep overbite and pointed chin	Short smooth philtrum Everted and thick lower lip Deep-set eyes Infraorbital crease Downward slanting of eyes Low set ears Mandibular retrognathia Crowding and retained deciduous teeth High arched palate with narrow vault Wide overjet, deep overbite and pointed chin	Smooth philtrum Mildly upturned nares Everted lower lip	Smooth philtrum Everted lower lip Hypodontia	Smooth philtrum Everted lower lip	ND	Smooth philtrum	Smooth philtrum	Smooth philtrum Everted lower lip Hypodontia Conical shaped teeth
CNS abnormality found by MRI	None	None	None	ND	ND	ND	Generalized atrophy Enlargement of ventricles	ND	none
Others	Severe sensorineural hearing loss	–	Hearing loss	–	–	–	Hepatomegaly	–	–

ND not determined, *OFC* occipitofrontal circumference, *SD* standard deviation

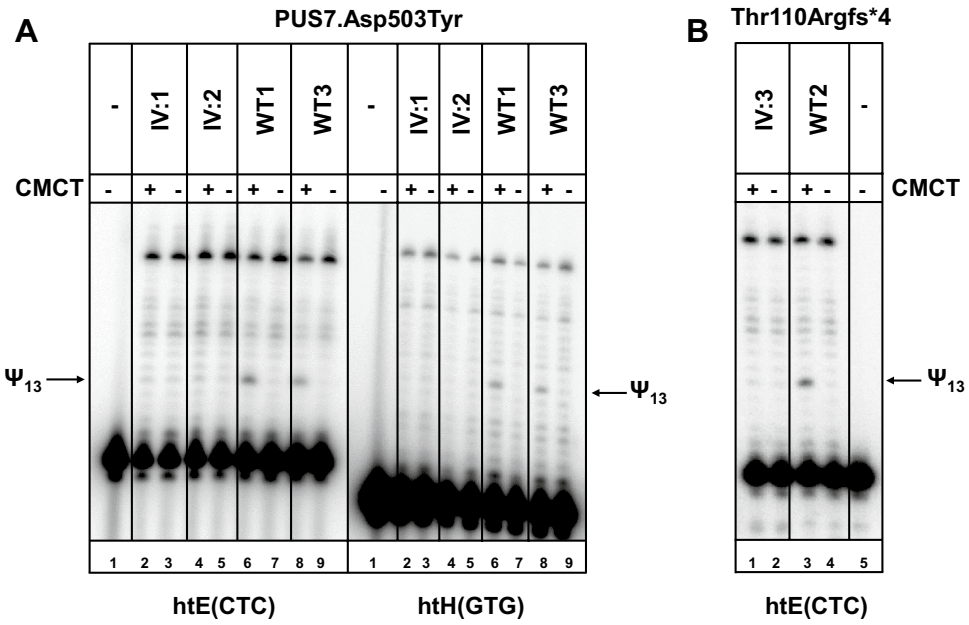

Fig. 2 LCLs from patients with PUS7 mutations have reduced levels of Ψ_{13} in tRNAs. LCLs from patients (IV:1, IV:2, IV:3) and controls (WT 1, WT 2, WT 3) were grown as described and bulk RNA was extracted, modified with CMCT, and analyzed for Ψ_{13} by primer extension. The reverse transcription pauses corresponding to Ψ_{13} are marked by arrows. **a** Ψ_{13} is not detected in $tRNA^{Glu(CTC)}$ and $tRNA^{His(GTG)}$ of LCLs from patients with a PUS7. Asp503Tyr mutation. **b** LCLs from patients with a PUS7. Thr110Argfs*4 mutation lack detectable Ψ_{13} in $tRNA^{Glu(CTC)}$

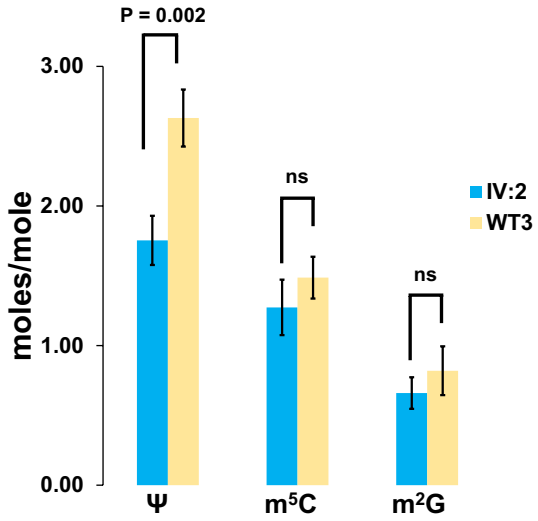

Fig. 3 $tRNA^{Val(AAC)}$ purified from LCLs of patients with the PUS7. Asp503Tyr mutation has reduced Ψ relative to that from control LCLs. LCLs were grown and tRNA was purified and analyzed for modifications, as described in "Materials and methods". Data derive from Table 2, showing that Ψ levels are reduced in patient LCLs (by 0.88 mol/mol), whereas levels of each of two other modifications are not

temperatures, due to rapid tRNA decay of $tRNA^{Val(AAC)}$ (Chernyakov et al. 2008). We found that expression of the yeast *pus7-D478Y* variant failed to detectably rescue the growth defect of the *pus7Δ trm8Δ* strain (Fig. 4). This result indicates that the yeast Pus7- D478Y variant is a complete loss of function mutation, and thus that the importance of the human Thr503 residue is conserved among eukaryotes.

Table 2 Analysis of modified nucleosides in $tRNA^{Val(AAC)}$ from control (WT3) and patient (IV:2) LCLs

Modification[a]	Moles expected	WT 3	IV:2
Ψ	3	2.63 ± 0.20	1.75 ± 0.18
m^5C	2	1.49 ± 0.15	1.27 ± 0.20
m^2G	1	0.82 ± 0.18	0.66 ± 0.11

[a]Mean and standard deviation based on three individual growths and RNA preparations

Discussion

There is a growing appreciation of the role of tRNA modification in human diseases based on revelations from Mendelian disorders (Ramos and Fu 2018; Torres et al. 2014). We previously reported that the most common single gene mutation associated with intellectual disability in Arabia was a point mutation in *ADAT3* (Alazami et al. 2013), which encodes an ortholog of yeast *TAD3*, a subunit of the complex required for I_{34} modification of substrate tRNAs (Gerber and Keller 1999). Furthermore, we showed that a founder mutation of *WDR4* impairs a highly conserved and specific (m^7G_{46}) methylation of tRNA with resulting severe encephalopathy and microcephaly (Shaheen et al. 2015). Additional Mendelian disorders include TRMT10A- and NSUN2-related syndromes

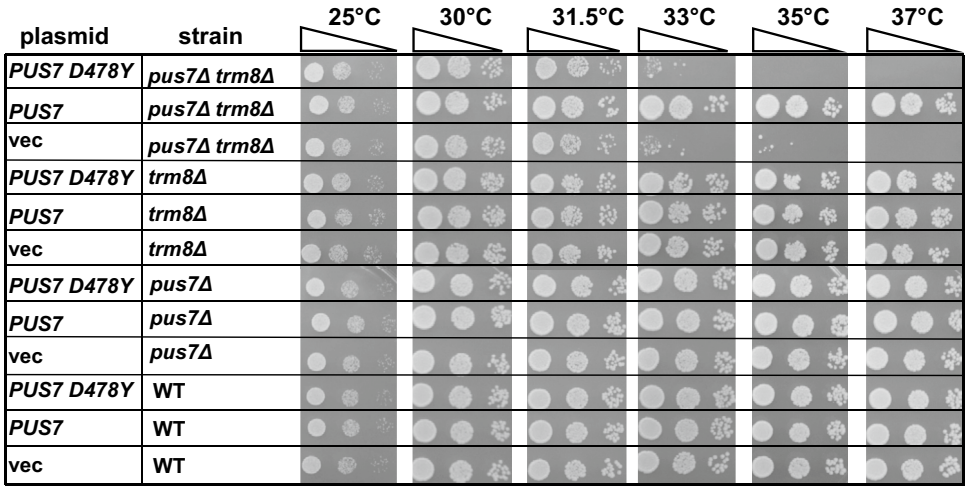

Fig. 4 Growth defect of an *S. cerevisiae trm8Δ pus7Δ* mutant at high temperature is not complemented by expressing *pus7-D478Y*. Wild type and *trm8Δ pus7Δ* strains harboring [*CEN URA3* P_{PUS7}-*pus7-D503Y*] or vector as indicated were grown overnight in S-Ura medium containing dextrose, diluted to OD600 of approximately 0.2 and serially diluted tenfold, and then 2 µL was spotted onto YPD media, followed by incubation for 3 days at temperatures as indicated

of intellectual disability, microcephaly, and short stature (Fahiminiya et al. 2013; Gillis et al. 2014; Igoillo-Esteve et al. 2013; Martinez et al. 2012). *TRMT10A* is the likely human homolog of yeast *TRM10* required for m^1G_9 modification (Jackman et al. 2003), while *NSUN2* is required for m^5C modification of body residues 48, 49, and 50 in mammals, as well as C_{34} of the anticodon (Blanco et al. 2014; Martinez et al. 2012).

Pseudouridine is the most abundant PTM of non-coding RNA observed to date across all domains of life (Cantara et al. 2010; Charette and Gray 2000). The additional NH group in pseudouridine at position 3 permits additional hydrogen bonding with other molecules, and this is thought to play a role in increasing the stability of RNA (Davis 1995; Spenkuch et al. 2014). In human tRNAs, pseudouridines are found at 13 different positions (residues 13, 20a, 20b, 31, 32, 27, 28, 35, 38, 39, 54, 55, and e2), and different pseudouridylases are required for modification at each of the different sites or sets of sites. Despite the abundance of this PTM of tRNA, its physiological relevance in humans has been limited to the reported phenotypes associated with mutations in *PUS1* and *PUS3* (Fernandez-Vizarra et al. 2007; Shaheen et al. 2016).

During the preparation of this manuscript, de Brouwer and colleagues described three families in which patients with intellectual disability, microcephaly and short stature harbored biallelic mutations in *PUS7* (de Brouwer et al. 2018). They also demonstrated that these mutations are associated with impaired pseudouridylation. The two families described here have different *PUS7* mutations, one of which is a point mutation in a highly conserved residue involved in a salt bridge in the *E. coli* TruD homolog (Kaya et al. 2004). While the phenotype we present in the three study patients supports the consistent involvement of cognition and postnatal brain growth and lack of epilepsy in PUS7 deficiency, it also suggests that other aspects are more variable. For example, index 1, whose mutation predicts a large PUS7 truncation, lacked the growth deficiency that was reported as a consistent feature by de Brouwer. In addition, we note the presence of sensorineural hearing loss in two of our patients. Unfortunately, the latter feature was not specifically commented on by de Brouwer, so it remains to be seen how common this, and indeed, other, clinical features are in *PUS7*-related syndrome.

We and others have previously emphasized the predilection of Mendelian diseases caused by tRNA modification genes to CNS involvement and how this suggests the vulnerability of the brain to any perturbation of tRNA modification, presumably through its deleterious effect on protein synthesis (Kirchner and Ignatova 2015; Ramos and Fu 2018; Shaheen et al. 2015; Torres et al. 2014). Indeed, a number of recent reviews have emphasized the emerging role of protein translation in neurological disorders in view of the expanding list of neurodevelopmental disorders caused by mutations in various components of protein translation and its regulation (Kapur and Ackerman 2018; Tahmasebi et al. 2018). Although the benefit of discovering these disease-gene links, including the one described in this study, is currently limited to establishing an accurate molecular diagnosis and prevention through informed reproductive choices, it is likely that these revelations will inform the development of therapeutics in the future.

In conclusion, we confirm that biallelic *PUS7* mutations in humans produce a syndrome of intellectual disability, progressive microcephaly and other variable features. The accompanying consistent defect in pseudouridylation provides hints at the potential pathogenesis of this syndrome. In addition, this may also serve as a very helpful assay for the proper classification of variants of unknown significance that will inevitably be encountered in this gene as exome/genome sequencing of children with intellectual disability will incorporate it in their annotation.

Acknowledgements We thank the study family for their enthusiastic participation. We also thank Mais Hashem, Niema Ibrahim and Firdous Abdulwahab for their help in coordinating the recruitment of the families and the Sequencing and Genotyping Core Facilities at KFSHRC for their technical help. This work was supported by the King Salman Center for Disability Research (F.S.A.), the Saudi Human Genome Program (F.S.A.), and by National Institutes of Health grant GM052347 (E.M.P.). M.T. was partially supported by NIH Training Grant in Cellular, Biochemical, and Molecular Sciences GM068411.

Compliance with ethical standards

Conflict of interest Authors declare no conflict of interest.

References

Alazami AM, Hijazi H, Al-Dosari MS, Shaheen R, Hashem A, Aldahmesh MA, Mohamed JY, Kentab A, Salih MA, Awaji A, Masoodi TA, Alkuraya FS (2013) Mutation in ADAT3, encoding adenosine deaminase acting on transfer RNA, causes intellectual disability and strabismus. J Med Genet 50(7):425–430

Alkuraya FS (2013) The application of next-generation sequencing in the autozygosity mapping of human recessive diseases. Hum Genet 132:1197–1211

Andrew TY, Ge J, Yu Y-T (2011) Pseudouridines in spliceosomal snRNAs. Protein Cell 2:712–725

Bakin A, Ofengand J (1993) Four newly located pseudouridylate residues in Escherichia coli 23S ribosomal RNA are all at the peptidyltransferase center: analysis by the application of a new sequencing technique. Biochemistry 32:9754–9762

Behm-Ansmant I, Urban A, Ma X, Yu Y-T, Motorin Y, Branlant C (2003) The *Saccharomyces cerevisiae* U2 snRNA: pseudouridine-synthase Pus7p is a novel multisite–multisubstrate RNA: Ψ-synthase also acting on tRNAs. RNA 9:1371–1382

Blanco S, Dietmann S, Flores JV, Hussain S, Kutter C, Humphreys P, Lukk M, Lombard P, Treps L, Popis M, Kellner S, Holter SM, Garrett L, Wurst W, Becker L, Klopstock T, Fuchs H, Gailus-Durner V, Hrabe de Angelis M, Karadottir RT, Helm M, Ule J, Gleeson JG, Odom DT, Frye M (2014) Aberrant methylation of tRNAs links cellular stress to neuro-developmental disorders. EMBO J 33(18):2020–2039

Boccaletto P, Machnicka MA, Purta E, Piątkowski P, Bagiński B, Wirecki TK, de Crécy-Lagard V, Ross R, Limbach PA, Kotter A (2017) MODOMICS: a database of RNA modification pathways. 2017 update. Nucleic Acids Res 46:D303–D307

Branlant C, Krol A, Machatt MA, Pouyet J, Ebel J-P, Edwards K, Kössel H (1981) Primary and secondary structures of *Escherichia coli* MRE 600 23S ribosomal RNA. Comparison with models of secondary structure for maize chloroplast 23S rRNA and for large portions of mouse and human 16S mitochondrial rRNAs. Nucleic Acids Res 9:4303–4324

Cantara WA, Crain PF, Rozenski J, McCloskey JA, Harris KA, Zhang X, Vendeix FA, Fabris D, Agris PF (2011) The RNA modification database, RNAMDB: 2011 update. Nucleic Acids Res 39:D195–D201

Carlile TM, Rojas-Duran MF, Zinshteyn B, Shin H, Bartoli KM, Gilbert WV (2014) Pseudouridine profiling reveals regulated mRNA pseudouridylation in yeast and human cells. Nature 515:143

Charette M, Gray MW (2000) Pseudouridine in RNA: what, where, how, and why. IUBMB Life 49:341–351

Chernyakov I, Whipple JM, Kotelawala L, Grayhack EJ, Phizicky EM (2008) Degradation of several hypomodified mature tRNA species in *Saccharomyces cerevisiae* is mediated by Met22 and the 5′–3′ exonucleases Rat1 and Xrn1. Genes Dev 22:1369–1380

Cohn WE (1959) 5-Ribosyl uracil, a carbon-carbon ribofuranosyl nucleoside in ribonucleic acids. Biochim Biophys Acta 32:569–571

Cohn WE, Volkin E (1951) Nucleoside-5′-phosphates from ribonucleic acid. Nature 167:483

Davis DR (1995) Stabilization of RNA stacking by pseudouridine. Nucleic Acids Res 23:5020–5026

de Brouwer APM, Abou Jamra R, Kortel N, Soyris C, Polla DL, Safra M, Zisso A, Powell CA, Rebelo-Guiomar P, Dinges N, Morin V, Stock M, Hussain M, Shahzad M, Riazuddin S, Ahmed ZM, Pfundt R, Schwarz F, de Boer L, Reis A, Grozeva D, Raymond FL, Riazuddin S, Koolen DA, Minczuk M, Roignant JY, van Bokhoven H, Schwartz S (2018) Variants in PUS7 cause intellectual disability with speech delay, microcephaly, short stature, and aggressive behavior. Am J Hum Genet 103:1045–1052

Endres L, Dedon PC, Begley TJ (2015) Codon-biased translation can be regulated by wobble-base tRNA modification systems during cellular stress responses. RNA Biol 12:603–614

Fahiminiya S, Almuriekhi M, Nawaz Z, Staffa A, Lepage P, Ali R, Hashim L, Schwartzentruber J, Abu Khadija K, Zaineddin S, Gamal H, Majewski J, Ben-Omran T (2013) Whole exome sequencing unravels disease-causing genes in consanguineous families in Qatar. Clin Genet 86(2):134–141

Fernandez-Vizarra E, Berardinelli A, Valente L, Tiranti V, Zeviani M (2007) Nonsense mutation in pseudouridylate synthase 1 (PUS1) in two brothers affected by myopathy, lactic acidosis and sideroblastic anaemia (MLASA). J Med Genet 44:173–180

Gerber AP, Keller W (1999) An adenosine deaminase that generates inosine at the wobble position of tRNAs. Science 286:1146–1149

Gillis D, Krishnamohan A, Yaacov B, Shaag A, Jackman JE, Elpeleg O (2014) TRMT10A dysfunction is associated with abnormalities in glucose homeostasis, short stature and microcephaly. J Med Genet 51:581–586

Grosjean H, Sprinzl M, Steinberg S (1995) Posttranscriptionally modified nucleosides in transfer RNA: their locations and frequencies. Biochimie 77:139–141

Hoernes TP, Hüttenhofer A, Erlacher MD (2016) mRNA modifications: Dynamic regulators of gene expression? RNA Biol 13:760–765

Huang C, Karijolich J, Yu Y-T (2016) Detection and quantification of RNA 2′-O-methylation and pseudouridylation. Methods 103:68–76

Igoillo-Esteve M, Genin A, Lambert N, Desir J, Pirson I, Abdulkarim B, Simonis N, Drielsma A, Marselli L, Marchetti P, Vanderhaeghen P, Eizirik DL, Wuyts W, Julier C, Chakera AJ, Ellard S, Hattersley AT, Abramowicz M, Cnop M (2013) tRNA methyltransferase homolog gene TRMT10A mutation in young onset diabetes and primary microcephaly in humans. PLoS Genet 9:e1003888

Jackman JE, Alfonzo JD (2013) Transfer RNA modifications: nature's combinatorial chemistry playground. Wiley Interdiscip Rev RNA 4:35–48

Jackman JE, Montange RK, Malik HS, Phizicky EM (2003) Identification of the yeast gene encoding the tRNA m1G methyltransferase responsible for modification at position 9. RNA 9:574–585

Kapur M, Ackerman SL (2018) mRNA translation gone awry: translation fidelity and neurological disease. Trends Genet 34:218–231

Kaya Y, Del Campo M, Ofengand J, Malhotra A (2004) Crystal structure of TruD, a novel pseudouridine synthase with a new protein fold. J Biol Chem 279:18107–18110

Kirchner S, Ignatova Z (2015) Emerging roles of tRNA in adaptive translation, signalling dynamics and disease. Nat Rev Genet 16:98

Li X, Zhu P, Ma S, Song J, Bai J, Sun F, Yi C (2015) Chemical pulldown reveals dynamic pseudouridylation of the mammalian transcriptome. Nat Chem Biol 11:592

Lovejoy AF, Riordan DP, Brown PO (2014) Transcriptome-wide mapping of pseudouridines: pseudouridine synthases modify specific mRNAs in *S. cerevisiae*. PLoS One 9:e110799

Martinez FJ, Lee JH, Lee JE, Blanco S, Nickerson E, Gabriel S, Frye M, Al-Gazali L, Gleeson JG (2012) Whole exome sequencing identifies a splicing mutation in NSUN2 as a cause of a Dubowitz-like syndrome. J Med Genet 49:380–385

Motorin Y, Helm M (2010) tRNA stabilization by modified nucleotides. Biochemistry 49:4934–4944

Ramos J, Fu D (2018) The emerging impact of tRNA modifications in the brain and nervous system. Biochim Biophys Acta Gene Regul Mech. https://doi.org/10.1016/j.bbagrm.2018.11.007

Schattner P, Barberan-Soler S, Lowe TM (2006) A computational screen for mammalian pseudouridylation guide H/ACA RNAs. RNA 12:15–25

Schwartz S, Bernstein DA, Mumbach MR, Jovanovic M, Herbst RH, León-Ricardo BX, Engreitz JM, Guttman M, Satija R, Lander ES (2014) Transcriptome-wide mapping reveals widespread dynamic-regulated pseudouridylation of ncRNA and mRNA. Cell 159:148–162

Shaheen R, Abdel-Salam GM, Guy MP, Alomar R, Abdel-Hamid MS, Afifi HH, Ismail SI, Emam BA, Phizicky EM, Alkuraya FS (2015) Mutation in WDR4 impairs tRNA m 7 G 46 methylation and causes a distinct form of microcephalic primordial dwarfism. Genome Biol 16:210

Shaheen R, Han L, Faqeih E, Ewida N, Alobeid E, Phizicky EM, Alkuraya FS (2016) A homozygous truncating mutation in PUS3 expands the role of tRNA modification in normal cognition. Hum Genet 135:707–713

Sherman F (1991) Getting started with yeast. Methods Enzymol 194:3–21

Spenkuch F, Motorin Y, Helm M (2014) Pseudouridine: still mysterious, but never a fake (uridine)! RNA Biol 11:1540–1554

Tahmasebi S, Khoutorsky A, Mathews MB, Sonenberg N (2018) Translation deregulation in human disease. Nat Rev Mol Cell Biol 19:791–807

Torres AG, Batlle E, de Pouplana LR (2014) Role of tRNA modifications in human diseases. Trends Mol Med 20:306–314

Zhao BS, Roundtree IA, He C (2017) Post-transcriptional gene regulation by mRNA modifications. Nat Rev Mol Cell Biol 18:31